Atmospheric
Chemistry
and Physics
Discussions

1  **Nitrate radical oxidation of γ-terpinene: hydroxy nitrate, total organic nitrate, and**
2  **secondary organic aerosol yields**

3  Jonathan H. Slade[1*], Chloé de Perre[2], Linda Lee[2], and Paul B. Shepson[1,3]

4  [1]Department of Chemistry, Purdue University, West Lafayette, IN 47907

5  [2]Department of Agronomy, Purdue University, West Lafayette, IN 47907

6  [3]Department of Earth, Atmospheric, and Planetary Sciences, Purdue University, West Lafayette,
7  IN 47907

8  [*]Corresponding author: jslade@purdue.edu

9    **Abstract**

10    Polyolefinic monoterpenes represent a potentially important but understudied source of

11    organic nitrates (ON) and secondary organic aerosol (SOA) following oxidation due to their high

12    reactivity and propensity for multi-stage chemistry. Recent modeling work suggests that the

13    oxidation of polyolefinic γ-terpinene can be the dominant source of nighttime ON in a mixed

14    forest environment. However, the ON yields, aerosol partitioning behavior, and SOA yields from

15    γ-terpinene oxidation by the nitrate radical ($NO_3$), an important nighttime oxidant, have not been

16    determined experimentally. In this work, we present a comprehensive experimental investigation

17    of the total (gas + particle) ON, hydroxy nitrate, and SOA yields following γ-terpinene oxidation

18    by $NO_3$. Under dry conditions, the hydroxy nitrate yield = 4(+1/-3)%, total ON yield = 14(+3/-

19    2)%, and SOA yield ≤ 10% under atmospherically-relevant particle mass loadings, similar to

20    those for α-pinene + $NO_3$. Using a chemical box model, we show that the measured

21    concentrations of $NO_2$ and γ-terpinene hydroxy nitrates can be reliably simulated from α-pinene

22    + $NO_3$ chemistry. This suggests that $NO_3$ addition to either of the two internal double bonds of γ-

23    terpinene primarily decomposes forming a relatively volatile keto–aldehyde, reconciling the

24    small SOA yield observed here and for other internal olefinic terpenes. Based on aerosol

25    partitioning analysis and identification of speciated particle-phase ON applying high-resolution

26    liquid chromatography–mass spectrometry, we estimate that a significant fraction of the particle-

27    phase ON has the hydroxy nitrate moiety. This work greatly contributes to our understanding of

28    ON and SOA formation from polyolefin monoterpene oxidation, which could be important in the

29    northern continental U.S. and Midwest, where polyolefinic monoterpene emissions are greatest.

30

Atmospheric
Chemistry
and Physics
Discussions

Open Access

## 1. Introduction

31

32      The oxidation of volatile organic compounds (VOCs) is a major pathway in the

33      production of secondary organic aerosol (SOA), which can represent up to ~60% of the total

34      submicron aerosol mass, depending on location [*Glasius and Goldstein*, 2016; *Hallquist et al.*,

35      2009; *Riipinen et al.*, 2012]. Aerosols impact climate by scattering and absorbing radiation as

36      well as modifying cloud optical properties, and can adversely affect human health [*Stocker et al.*,

37      2013]. A large fraction of the total OA budget derives from the oxidation of *biogenic* VOCs

38      (BVOCs), including isoprene ($C_5H_8$) and monoterpenes ($C_{10}H_{16}$) [*Hallquist et al.*, 2009;

39      *Spracklen et al.*, 2011]. Together, these naturally emitted compounds account for ~60% of the

40      global BVOC budget [*Goldstein and Galbally*, 2007; *Guenther et al.*, 1995]. In particular,

41      monoterpenes, comprising ~11% of the total global BVOC emissions [*Guenther*, 2002],

42      represent a viable source of SOA following oxidation [*Griffin et al.*, 1999; *A Lee et al.*, 2006].

43      However, atmospheric models routinely underestimate the global SOA burden [*Kokkola et al.*,

44      2014], causing a potential order of magnitude error when predicting global aerosol forcing

45      [*Goldstein and Galbally*, 2007], and thus the sources and mechanisms responsible for SOA

46      formation require further study.

47      VOC oxidation produces an array of semi-volatile organic aerosol precursors, including

48      organic nitrates ($RONO_2$), herein referred to as "ON", in the presence of $NO_x$ (i.e., $NO+NO_2$)

49      [*Darnall et al.*, 1976; *Kroll and Seinfeld*, 2008; *Rollins et al.*, 2012; *Rollins et al.*, 2010b]. By

50      sequestering $NO_x$, ON can perturb ozone concentrations globally [*Squire et al.*, 2015]. Moreover,

51      as $NO_x$ concentrations are expected to decrease in the future [*von Schneidemesser et al.*, 2015],

52      ambient concentrations of $NO_x$ and thus $O_3$ will become increasingly sensitive to ON formation

53      [*Tsigaridis and Kanakidou*, 2007]. Monoterpenes contribute significantly to the formation of ON

Atmospheric
Chemistry
and Physics
Discussions

Open Access

EGU

54    and SOA, especially during nighttime in the presence of nitrate radicals ($NO_3$), when isoprene

55    concentrations are negligible and the photolytic and NO reaction sinks of $NO_3$ are cut off

56    [*Rollins et al.*, 2012]. It is estimated that monoterpene oxidation by $NO_3$ may account for more

57    than half of the monoterpene-derived SOA in the U.S., suggesting that ON is a dominant SOA

58    precursor [*Pye et al.*, 2015]. However, their formation mechanisms and yields following

59    oxidation by $NO_3$ are not as well constrained as those from OH and $O_3$ oxidation [*Hoyle et al.*,

60    2011], and previous studies have focused on the $NO_3$ oxidation of only a few monoterpenes [*Fry*

61    *et al.*, 2014], but almost exclusively on mono-olefinic terpenes such as α- and β-pinene

62    [*Berkemeier et al.*, 2016; *Boyd et al.*, 2015; *Fry et al.*, 2009; *Spittler et al.*, 2006; *Wangberg et*

63    *al.*, 1997]. An important detail is the relative amount of hydroxy nitrates produced, as the -OH

64    group contributes greatly to water solubility [*Shepson et al.*, 1996], and uptake into aqueous

65    aerosol followed by continuing chemistry in the aqueous phase, which can be an important

66    mechanism for SOA production [*Carlton and Turpin*, 2013].

67        A major challenge regarding our understanding of SOA formation from monoterpene

68    oxidation is that there are several isomers of monoterpenes with very different structural

69    characteristics that can exhibit very different yields of SOA following oxidation [*Fry et al.*,

70    2014; *Ziemann and Atkinson*, 2012]. For example, the SOA mass yield from the $NO_3$ oxidation

71    of α-pinene, which contains one endocyclic double bond, is ~0% under atmospherically relevant

72    particle mass loadings, whereas that from β-pinene, which contains one terminal double bond, is

73    33% under the same experimental conditions [*Fry et al.*, 2014]. Limonene, with one tertiary

74    endo- and one terminal exocyclic double bond, also exhibits relatively larger SOA mass yields

75    following oxidation by $NO_3$ [*Fry et al.*, 2014; *Spittler et al.*, 2006]. Because $NO_3$ oxidation of α-

76    pinene primarily leads to tertiary peroxy radical formation [*Wangberg et al.*, 1997], the initially

Atmospheric
Chemistry
and Physics
Discussions

Open Access

EGU

77    formed alkoxy radical decomposes, releasing $NO_2$ and forming a keto–aldehyde, which has

78    higher saturation vapor pressure compared to its ON analogue [*Pankow and Asher*, 2008]. In

79    contrast, $NO_3$ addition to the terminal double bonds of β-pinene and limonene lead to more stable

80    ON species with lower saturation vapor pressure that partition to the aerosol phase. SOA yields

81    have also been shown to be strongly dependent on the total (gas + particle) yield of ON.  Owing

82    to their low saturation vapor pressures, multifunctional ON such as the hydroxy nitrates, are

83    thought to contribute significantly to SOA formation [*B H Lee et al.*, 2016; *Rollins et al.*, 2010a;

84    *Rollins et al.*, 2010b], but, for BVOCs, so far have only been measured in the eastern US

85    [*Grossenbacher et al.*, 2004; *B H Lee et al.*, 2016; *F Xiong et al.*, 2015]. These ON can undergo

86    aqueous-phase processing to form diols and organosulfates [*Jacobs et al.*, 2014; *Rindelaub et al.*,

87    2016; *Rindelaub et al.*, 2015; *Surratt et al.*, 2008], which not only affect saturation vapor

88    pressure and thus aerosol formation, but also represent a sink for $NO_x$ and affect the hygroscopic

89    properties of organic aerosol [*Suda et al.*, 2014]. However, considering there are only a limited

90    number of studies that have specifically investigated the yield of hydroxy nitrates, namely

91    following OH and $NO_3$ oxidation of isoprene [*Chen et al.*, 1998; *Lockwood et al.*, 2010; *F Xiong*

92    *et al.*, 2015] and α-pinene [*Rindelaub et al.*, 2015; *Wangberg et al.*, 1997], further measurements

93    of their yields and role in aerosol formation from the oxidation of other terpenoids is critical.

94        In the southeastern U.S., α- and β-pinene tend to dominate monoterpene emissions

95    [*Geron et al.*, 2000], and their potential for ON and SOA formation are better understood [*Ayres*

96    *et al.*, 2015; *B H Lee et al.*, 2016]. However, in other regions of the U.S., polyolefinic

97    monoterpenes such as terpinene, ocimene, and limonene can be present in much greater

98    proportions than in the southeastern US, which may be in part due to the relatively smaller

99    abundance of the α- and β-pinene emitter southern pine, but also more polyolefinic monoterpene

100   emitters, including *Juniperus scopulorum*, a common cedar and γ-terpinene emitter in the

101   Midwestern US [*Geron et al.*, 2000]. In particular, model simulations suggest that the oxidation

102   of γ-terpinene, comprising two substituted endocyclic double bonds, can contribute as much as

103   α- and β-pinene to nighttime organic nitrate production in a mixed northern hardwood forest

104   [*Pratt et al.*, 2012]. Those authors also showed that $NO_3$ reaction with BVOCs is important in

105   the daytime. However, the ON and SOA yields following $NO_3$ oxidation of γ-terpinene have not

106   been determined in laboratory studies.

107   Here we present a comprehensive laboratory investigation of the hydroxy nitrate, total

108   gas and particle-phase ON, and SOA yields from the $NO_3$ oxidation of γ-terpinene. For the

109   hydroxy nitrate yield experiments, a surrogate standard compound was synthesized [*Rindelaub et*

110   *al.*, 2016], enabling quantitative determination of its yield using a chemical ionization mass

111   spectrometer (CIMS). This work contributes to a broader understanding of SOA formation from

112   the oxidation of polyolefinic monoterpenes, and the role of $NO_3$ oxidation chemistry in the

113   sequestration of $NO_x$.

114

115   **2. Methods**

116   Yield experiments were conducted in a 5500 L all-Teflon photochemical reaction

117   chamber in the dark. Briefly, the chamber was cleaned by flushing several times with ultra-zero

118   (UZ) air in the presence of ultra-violet light. Experiments were conducted in a dry atmosphere

119   (relative humidity < 1%) and at ambient temperature (~295 K). A total of 13 independent yield

120   experiments were conducted over a range of initial γ-terpinene concentrations in the presence of

121   $N_2O_5$ with and without $(NH_4)_2SO_4$ seed particles. $N_2O_5$ was produced in a dried glass vessel and

122  crystallized at 195 K in a custom-made glass trap following thermal equilibrium with $NO_2$ and

123  $O_3$, as indicated in reactions (1) and (2) below.

124  $$O_3 \quad + \quad NO_2 \quad \rightarrow \quad NO_3 \quad + \quad O_2 \qquad (1)$$

125  $$NO_3 \quad + \quad NO_2 \quad \leftrightarrow \quad N_2O_5 \qquad (2)$$

126  First, the BVOC was transferred to the chamber with UZ air via injection through a heated glass

127  inlet and polytetrafluoroethylene line. For the seeded experiments, $(NH_4)_2SO_4$ particles were

128  generated by passing an aqueous solution through a commercial atomizer (Model 3076, TSI,

129  Inc.) and subsequently dried through a diffusion dryer prior to entering the reaction chamber.

130  The seed particles were polydisperse with a range in the geometric mean diameter, $D_{p,g}$, of 57 nm

131  to 94 nm and geometric standard deviation, $\sigma_g$, of 1.39 to 1.91. Total seed number and mass

132  concentrations were in the range $0.61\text{-}5.15 \times 10^4$ $cm^{-3}$ and 8-48 µg $m^{-3}$, respectively, assuming a

133  particle density of 1.2 g $cm^{-3}$. Yield experiments were initiated (time = 0) by injecting $N_2O_5$ into

134  the chamber with a flow of UZ air over the crystalline $N_2O_5$. The reactants were allowed to

135  continuously mix in the chamber with a fan, and the reaction was terminated when no less than

136  10% of the γ-terpinene remained to limit secondary particle-phase or heterogeneous $NO_3$

137  chemistry.

138      Real-time measurements were made using several instruments: γ-terpinene

139  concentrations were measured with a gas chromatograph-flame ionization detector (GC-FID;

140  HP-5890 Series II), which was calibrated using a commercial γ-terpinene standard dissolved in

141  cyclohexane. $NO_2$ concentrations were measured with a custom-built chemiluminescence $NO_x$

142  analyzer [*Lockwood et al.*, 2010], and a scanning mobility particle sizer (SMPS; Model 3062,

143  TSI, Inc.) was used to determine size-resolved particle mass concentrations. No direct

144  concentration measurements of $NO_3$ were made. The hydroxy nitrates were measured online

Atmospheric
Chemistry
and Physics
Discussions

145    continuously using an iodide-adduct chemical ionization mass spectrometer (CIMS) [*F Xiong et*

146    *al.*, 2015; *F L Z Xiong et al.*, 2016]. To quantify the production of monoterpene hydroxy nitrates,

147    the CIMS was calibrated with a purified standard of an α-pinene-derived hydroxy nitrate

148    synthesized in-house via nitrification of α-pinene oxide (Sigma–Aldrich, 97%) using

149    $Bi(NO_3)_3 \cdot 5H_2O$ [*Rindelaub et al.*, 2016]. The concentration of the purified hydroxy nitrate was

150    verified via two complementary methods: ^{1}HNMR and FTIR, and the structure was verified

151    using ^{13}C-NMR, as presented in the supplementary information of *Rindelaub et al.* [2016]. The

152    total ON yields and concentration of the standard were determined via FTIR measurement of the

153    asymmetric $-NO_2$ stretch located at ~1640 $cm^{-1}$ using tetrachloroethylene (Sigma–Aldrich,

154    HPLC grade, ≥99.9%) as the solvent [*Rindelaub et al.*, 2015]. The total gas-phase ON yields

155    were determined with FTIR following the sampling of chamber air through an annular denuder

156    (URG-200) coated with XAD-4 resin and extraction from the denuder walls with

157    tetrachloroethylene as in a previous study [*Rindelaub et al.*, 2015]. Aerosol particles were

158    collected on 47 mm Teflon filters (1 μm pore size) housed in a cartridge connected to the

159    denuder exit. The collection efficiency of the denuder walls for gas-phase organic nitrates was

160    determined to be >98% based on measurements of the concentration of 2-ethyl-hexyl-nitrate

161    (Sigma–Aldrich, 97%) before and after the denuder with the GC-FID. The particle transmission

162    efficiency was determined to be >98% by measuring the number concentration of particles

163    before and after the denuder with the SMPS.

164         Wall loss and dilution corrections were applied to both the SOA and ON yields

165    accounting for the time required to sample through the denuder. Following several of the

166    experiments, the SOA concentration was measured as a function of reaction time with the wall

167    with an average wall loss rate constant, $k_{wall,SOA} = 9 \times 10^{-5}$ $s^{-1}$. The gas-phase ON wall loss rate

Atmospheric
Chemistry
and Physics
Discussions

168    was determined based on the evolution of the CIMS-derived monoterpene hydroxy nitrate

169    (M=$C_{10}H_{17}NO_4$) signal ([M+I]$^-$; $m/z$ = 342) following an experiment, in which we obtained $k_{ONg}$

170    = $2 \times 10^{-5}$ s$^{-1}$, as shown in Fig. S1.

171        Selected filter extracts from two separate chamber experiments were analyzed for their

172    chemical composition via ultra-performance liquid chromatography electrospray ionization time-

173    of-flight tandem mass spectrometry (UPLC-ESI-ToF-MS/MS, Sciex 5600+ TripleToF with

174    Shimadzu 30 series pumps and autosampler) to identify potential ON species in the particle

175    phase from γ-terpinene oxidation by $NO_3$. The samples were first dried with ultra-high purity

176    nitrogen and then extracted with a 1:1 v:v solvent mixture of HPLC-grade methanol and 0.1%

177    acetic acid in nanopure $H_2O$, which has been used successfully as a solvent system for

178    identifying multifunctional organonitrate and organosulfate species [*Surratt et al.*, 2008].

179    **3.    Results and Discussion**

180    *3.1. SOA yields*

181        Mass-dependent SOA yields ($Y_{SOA}$) were derived from both seeded and unseeded

182    experiments and defined here as the change in aerosol mass concentration (ΔM in μg m$^{-3}$)

183    relative to the concentration of BVOC consumed (ΔBVOC in μg m$^{-3}$), i.e., $Y_{SOA} = \Delta M / \Delta BVOC$.

184    ΔM was derived from individual SOA growth curves as shown in Fig. 1. Here the initial mass is

185    defined as the average SMPS-derived particle mass in the chamber prior to $N_2O_5$ injection, and

186    the final mass is derived from the maximum of the SOA growth curve when ΔBVOC stabilizes,

187    as shown in Fig. S2. Note that under these experimental conditions, SOA formation occurs

188    rapidly, limited on the short end by the thermal decomposition e-folding lifetime of $N_2O_5$ (~30 s

189    at 295 K) and the e-folding lifetime of $NO_3$ reaction with γ-terpinene (few milliseconds assuming

190    a rate constant of $2.9 \times 10^{-11}$ cm$^3$ molecule$^{-1}$ s$^{-1}$), and on the long end by the time scale for

Atmospheric
Chemistry
and Physics
Discussions

191    heterogeneous uptake of $N_2O_5$ of several hours assuming an uptake coefficient at low relative

192    humidity of $10^{-4}$ [*Abbatt et al.*, 2012].

193        $Y_{SOA}$ with and without seed particles as a function of particle mass loading are depicted in

194    Fig. 2. The curve shows that under low mass loadings, the yields are less than under high mass

195    loadings, indicative of absorptive partitioning [*Hao et al.*, 2011; *Odum et al.*, 1996]. To model

196    the measured $Y_{SOA}$ as a function of particle mass loading, we apply an absorptive partitioning

197    model following the method of *Odum et al.* [1996], as shown in Eq. (1).

198
$$Y_{SOA} = M_0 \sum_i \left( \frac{\alpha_i K_{om,i}}{1 + K_{om,i} M_0} \right)$$

199    Here, $\alpha_i$ is a proportionality constant describing the fraction of product $i$ in the aerosol phase, $M_0$

200    is the aerosol mass concentration, and $K_{om,i}$ is the absorptive partitioning coefficient of the

201    absorbing material. Assuming a two-product model, the best fit values are $\alpha_1 = 0.94$, $K_{om,1} =$

202    $7.9 \times 10^{-4}$, $\alpha_2 = 0.33$, and $K_{om,1} = 2.6 \times 10^{-2}$. Extending this model to a conservative ambient mass

203    loading of 10 µg m$^{-3}$, characteristic of biogenic SOA-impacted environments [*Fry et al.*, 2014],

204    the SOA yield is ~10%. In contrast, at mass loadings >500 µg m$^{-3}$, which is more relevant in

205    highly polluted urban areas such as those along the coast of India [*Bindu et al.*, 2016], $Y_{SOA}$ can

206    be as large as ~50%. For comparison, $Y_{SOA}$ of other reaction systems applying the absorptive

207    partitioning values derived from those experiments are plotted along with our experimental data

208    in Fig. 2. The γ-terpinene + $NO_3$ $Y_{SOA}$ are significantly less than those involving β-pinene, an

209    important contributor to SOA formation predominately in the southeastern U.S [*Boyd et al.*,

210    2015]. However, at relatively low particle mass loadings, $Y_{SOA}$ for $NO_3$ + γ-terpinene is

211    comparable to those derived from the OH oxidation of γ-terpinene and α-pinene [*Griffin et al.*,

212    1999; *A Lee et al.*, 2006]. Interestingly, our measured $Y_{SOA}$ at comparable mass loadings are also

Atmospheric
Chemistry
and Physics
Discussions

213    within the reported range of $Y_{SOA}$ from the $NO_3$ oxidation of α-pinene of 0-16% (see *Fry et al.*

214    [2014] and references therein), which are relatively small compared to other monoterpene + $NO_3$

215    reaction systems, which range from 13% to 65% for β-pinene, limonene, and Δ-3-carene [*Fry et*

216    *al.*, 2014]. The studies reporting low $Y_{SOA}$ also report relatively low ON yields and high ketone

217    yields, suggesting that the $NO_3$ oxidation products of α-pinene, and likely γ-terpinene, are

218    sufficiently volatile and do not contribute significantly to SOA formation under atmospherically-

219    relevant aerosol mass loadings. In contrast, the experiments reporting higher $Y_{SOA}$ report

220    relatively greater ON/ketone yield ratios, with the exception of sesquiterpenes such as β-

221    caryophyllene, suggesting ON are important aerosol precursors.

222

223        *3.2. Organic nitrate yields*

224        ON can partition to the particle phase and contribute to SOA formation and mass growth.

225    However, measurements of their yields are limited and highly variable depending on the

226    composition of the reactive organic species and the type of oxidant [*Ziemann and Atkinson*,

227    2012]. Here we report the measured gas- and aerosol-phase ON yields, and the total (sum of gas

228    and aerosol ON) yield following γ-terpinene oxidation by $NO_3$. The ON yields ($Y_{ON}$) are defined

229    as the concentration of ON produced (ΔON) either in the gas or particle phases, relative to the

230    concentration of BVOC consumed, ΔBVOC, i.e., $Y_{ON} = ΔON/ΔBVOC$. In these experiments,

231    ΔBVOC was varied systematically by altering the concentration of $N_2O_5$ added to the chamber

232    and monitoring the change in BVOC concentration with the GC-FID. These experiments were

233    conducted both in the presence and absence of $(NH_4)_2SO_4$ seed aerosol particles and under dry

234    conditions, and corrected for wall losses and dilution.

235

Atmospheric
Chemistry
and Physics
Discussions

### 3.2.1. *Total gas-phase organic nitrate yield*

As indicated in Fig. 3, the concentration of total gas-phase ON ($ON_g$; determined via FT-IR) increases linearly as a function of ΔBVOC, independent of the presence or absence of the seed aerosol. By fitting both the unseeded and seeded data using linear regression, we derive a gas-phase molar ON yield ($Y_{ONg}$) of 11($\pm$1)%, where the relative uncertainty in the yield of ~9% is derived from the 95% confidence intervals (shown in dashed lines in Fig. 3) of the linear fit to the data, and accounting for the measurement uncertainties, shown as error bars. The similar yields with or without seed particles implies that after some uptake, the two cases might appear identical to the adsorbing molecules. However, $Y_{ONg}$ may be affected by secondary oxidation reactions. We estimate based on the relative rates of primary and secondary oxidation of other monoterpenes that secondary oxidation may decrease $ON_g$ by ~10% (i.e., $Y_{ONg}$ may be greater by 10%), suggesting that most of the $NO_3$ radicals were reacted with γ-terpinene. $Y_{ONg}$ observed here for γ-terpinene is considerably smaller than those measured from the $NO_3$ oxidation of limonene and β-pinene, but very similar to the yield from $NO_3$ oxidation of α-pinene [*Fry et al.*, 2014].

### 3.2.2. *Total particle-phase organic nitrate yield*

In general, particle-phase ON concentrations ($ON_p$) increase with increasing ΔBVOC as shown in Fig. 4, with a particle-phase ON yield ($Y_{ONp}$) from the slope of 3($\pm$1)%. Since there was no significant variability in $ON_p$ with and without seed aerosol, the slope (i.e., yield) is derived from a fit to both datasets. The greater spread in the $ON_p$ compared to $ON_g$ (see Fig. 3) as a function of ΔBVOC may be due to relatively lower ON yields, which were derived from signals close to the measured background noise of the FT-IR instrument. Under dry conditions, as in

Atmospheric
Chemistry
and Physics
Discussions

259   these experiments, the total ON yield (including particle phase) may be expected to be similar for

260   seeded and unseeded experiments [*Rindelaub et al.*, 2015]. However, while the relative humidity

261   during these experiments was minimal, it is possible that some particle-phase hydrolysis could

262   occur, aided by uptake of product $HNO_3$ by the particles [*Rindelaub et al.*, 2015]. Thus we

263   estimate an aerosol organic nitrate yield of 3 (+2/-1)%, based on the upper limit of the data

264   variability.

265

266      *3.3. Organic nitrate aerosol partitioning*

267      The sum of $ON_g + ON_p$ ($ON_t$) is plotted as a function of $\Delta BVOC$ in Fig. 5. Together, they

268   result in a total molar ON yield, $Y_{ONt} = 14(+3/-2)\%$, accounting for the potential loss of aerosol

269   phase ON as described previously, comparable to previously measured ON yields from the $NO_3$

270   oxidation of α-pinene of 10% [*Fry et al.*, 2014] and 14% [*Wangberg et al.*, 1997]. From the ratio

271   $Y_{ONp}/Y_{ONt}$, ~20% of the total ON produced from γ-terpinene + $NO_3$ partitioned to the particle

272   phase, for these relatively high aerosol mass loading conditions. Assuming an average ON molar

273   mass of 215 g mol$^{-1}$, representing a $C_{10}$-derived hydroxy nitrate [*Rindelaub et al.*, 2015], roughly

274   14% of the total aerosol mass is comprised of ON. Gas-to-particle partitioning depends strongly

275   on the molecule's equilibrium saturation vapor pressure and mass transfer kinetics [*Shiraiwa and*

276   *Seinfeld*, 2012]. The addition of nitrooxy and hydroxy groups, for example, can reduce the

277   equilibrium saturation vapor pressure by several orders of magnitude [*Capouet et al.*, 2008].

278   Molecules with saturation vapor pressures $>10^{-5}$ atm are almost exclusively in the gas phase,

279   whereas those below $10^{-13}$ atm are almost exclusively in the condensed phase [*Compernolle et*

280   *al.*, 2011]. We can estimate the saturation vapor pressure of the ON ($p_i^0$) based on the estimated

281   ON aerosol mass fraction ($\varepsilon_i^{aero}=0.14$) as given in Eq. (2) [*Valorso et al.*, 2011].

13

282

$$\varepsilon_i^{\text{aero}} = \frac{1}{1 + \dfrac{M_{\text{aero}}\gamma_i p_i^0}{C_{\text{aero}}\text{R}T}}$$

284

Here, $M_{\text{aero}}$ is the average particle molar mass, $\gamma_i$ is the activity coefficient of molecule "i", and

$C_{\text{aero}}$ is the aerosol mass concentration, R is the gas constant, and $T$ is temperature. Assuming

ideality, i.e., $\gamma_i=1$, $C_{\text{aero}}=838$ µg m$^{-3}$ (average of ΔM values from experiments listed in table 1),

and $M_{\text{aero}}=215$ g mol$^{-1}$, we derive a $p_i^0$ for ON of ~6×10$^{-7}$ atm or log$_{10}$ saturation concentration of

~4 µg m$^{-3}$, which for a semivolatile C$_{10}$-derived hydrocarbon is expected to have between two

and four oxygen atoms [*Donahue et al.*, 2011]. This estimated $p_i^0$ for ON is about an order of

magnitude greater than that calculated for the expected tertiary hydroxy and hydroperoxy nitrates

of γ-terpinene shown in Fig. 8 of 6.9×10$^{-8}$ atm and 3.9×10$^{-8}$ atm, respectively, using SIMPOL.1

[*Pankow and Asher*, 2008], suggesting that the ON$_p$ products of γ-terpinene likely comprise a

mixture of hydroperoxy and hydroxy nitrates, and other more volatile ON species, likely keto–

nitrates, e.g. as shown in Fig. 8 for the case of NO$_3$ addition to the more-substituted carbon. For

the keto–nitrate shown in Fig. 8, we calculate a $p_i^0$ value of 1.4×10$^{-6}$ atm, using SIMPOL,

roughly a factor of two greater than our estimate for the average for our aerosol. For comparison,

the keto–aldehyde presented in Fig. 8 (γ-terpinaldehyde) has a $p_i^0$ value of 0.092 atm, using

SIMPOL. As presented in the supplementary information, analysis of liquid extracts from filter

samples using UPLC-ESI-ToF-MS/MS operated in negative ion mode indicate the presence of

masses consistent with the first-generation hydroperoxy nitrate and second-generation di-

hydroxy di-nitrates in the aerosol phase, the latter of which may result from both gas- and

heterogeneous reactions that proceed at the unsubstituted olefinic C of a γ-terpinene hydroxy

Atmospheric
Chemistry
and Physics
Discussions

304    nitrate. Regardless, an aerosol mass fraction of ON of 14% is considerably less than that

305    obtained for other monoterpenes reacting with $NO_3$, with the exception of α-pinene [*Fry et al.*,

306    2014]. This could be a result of both production of mostly volatile ON species, in particular

307    keto–nitrates, and further reaction of the olefinic hydroxy nitrate in the aerosol phase. To verify

308    the potential role of hydroxy nitrates in SOA production from $NO_3$ + γ-terpinene as well as the

309    presence of other ON, the following section focuses on product identification of gas phase ON

310    species using CIMS and determination of gas phase hydroxy nitrate yields.

311

312    *3.4. CIMS product identification and hydroxy nitrate yields*

313    $NO_3$ reactions with VOCs lead to either abstraction of a hydrogen atom or addition to a

314    double bond. Since γ-terpinene has two double bonds with similar character, $NO_3$ likely has

315    equal probability of adding to either internal double bond. However, addition of $NO_3$ to either

316    one of the olefins is likely to form the more stable tertiary nitrooxy alkyl radical. Subsequent

317    addition of $O_2$ forms the β-nirooxyperoxy radical that can lead to an array of products, including

318    hydroxy nitrates, most likely from self or cross $RO_2\cdot$ + $RO_2\cdot$ reactions or isomerization [*Yeh and*

319    *Ziemann*, 2014; *Ziemann and Atkinson*, 2012]. $C_{10}$-derived hydroxy nitrates and other

320    multifunctional ON have been identified in field-sampled SOA particles, and for nighttime $ON_p$,

321    $C_{10}$-derived ON could account for approximately 10% of the organic aerosol mass during the

322    Southern Oxidant and Aerosol Study (SOAS) campaign in the U.S. southeast [*B H Lee et al.*,

323    2016; *Xu et al.*, 2015]. However, our current understanding of $C_{10}$-derived hydroxy nitrate yields

324    is limited to production via oxidation of α-pinene [*Wangberg et al.*, 1997]. Here we expand on

325    this by determining the hydroxy nitrate yield from γ-terpinene oxidation by $NO_3$ and identify

326    other potentially important ON species using CIMS.

Atmospheric
Chemistry
and Physics
Discussions

327     Figure 6 shows a typical CIMS mass spectrum following a chamber experiment involving

328     γ-terpinene oxidation by $NO_3$. Several larger molecular weight species are detected by the

329     iodide-adduct CIMS, including several masses in the range of $300 \leq m/z \leq 450$. Specifically, the

330     first-generation hydroxy nitrates are observed at $m/z = 342$ ($C_{10}H_{17}NO_4–I^-$). Several masses

331     follow, separated by 16 mass units, or addition of a single oxygen atom, whereby each new ON

332     has 15, 17, or 19 H atoms. Similar observations were made in the field during the SOAS

333     campaign for both $ON_g$ and $ON_p$ [*B H Lee et al.*, 2016], indicating the presence of highly-

334     functionalized ON. It is important to note that the products observed here are derived from a

335     single monoterpene, whereas the field ON measurements consist of products derived from all

336     ambient monoterpene oxidation. Other major peaks included those at $m/z = 340$, potentially

337     representing an iodide-adduct with either an aldehyde or keto–nitrate ($C_{10}H_{15}NO_4–I^-$), $m/z = 358$,

338     which may be indicative of an iodide-adduct with a hydroperoxy nitrate ($C_{10}H_{17}NO_5–I^-$), and

339     small but persistent peak at $m/z = 421$, potentially representing an iodide-adduct with a di-

340     hydroxy–di-nitrate ($C_{10}H_{18}N_2O_8–I^-$), which could be formed through second-generation

341     oxidation at the remaining unsubstituted carbon of the double bond on the first-generation

342     hydroxy nitrate. It is important to note that the CIMS sensitivity for each of these species is

343     likely different and depends on the polarity and acidity of the individual compound, which is

344     affected by the type and positions of the different functional groups [*B H Lee et al.*, 2016]. For

345     example, iodide-adduct CIMS is not particularly sensitive to aldehyde and carbonyl nitrates,

346     whereas more acidic and polar molecules such as hydroxy nitrates and carboxylic acids can

347     exhibit much greater sensitivity [*B H Lee et al.*, 2016]. Moreover, in general as the molecular

348     size and number of oxygenated groups increase (particularly –OH groups), the sensitivity also

Atmospheric
Chemistry
and Physics
Discussions

349     increases. Hence, without commercial or custom synthetic standards, no quantitative analysis of

350     the array of ON products could be reliably performed using this technique.

351         Here we determine the yield of γ-terpinene-derived hydroxy nitrates. Since there is no

352     commercially-available standard for the expected first-generation γ-terpinene hydroxy nitrate, we

353     use a synthetic olefinic hydroxy nitrate derived from α-pinene (structure shown in Fig. S4) for

354     quantitative analysis [*Rindelaub et al.*, 2016]. It is possible that the CIMS is less sensitive to this

355     nitrate compared to the more sensitive α,β-hydroxy nitrate structure expected of the first-

356     generation γ-terpinene hydroxy nitrates, similar to the differences in the CIMS sensitivity for

357     4,3-isoprene hydroxy nitrate (4,3-IN) and 1,4-IN [*F Xiong et al.*, 2015]. However, the use of an

358     olefinic hydroxy nitrate is consistent with that expected from γ-terpinene oxidation because of its

359     diolefinic character. As shown in Fig. 7, γ-terpinene-derived hydroxy nitrate concentrations

360     increase linearly over the range of ΔBVOC with a hydroxy nitrate yield defined from the slope

361     as 4(±1)%. Assuming the CIMS sensitivity for the γ-terpinene hydroxy nitrates may be a factor

362     of three greater than for our synthetic α-pinene-derived hydroxy nitrate, a more conservative

363     estimate of the γ-terpinene-derived hydroxy nitrate yield is 4(+1/-3)%. To our knowledge, the

364     only monoterpene hydroxy nitrate yield to have been quantified following $NO_3$ oxidation is 2-

365     hydroxypinan-3-nitrate, derived from α-pinene [*Wangberg et al.*, 1997]. In that study, the

366     hydroxy nitrate yield was determined using a combination of FT-IR and GC-ECD to be

367     5(±0.4)%, on the same order as the yield presented in this study for γ-terpinene using CIMS. 3-

368     oxopinan-2-nitrate ($C_{10}H_{15}NO_4$; 213 g mol$^{-1}$) and a short-lived, thermally unstable peroxy nitrate

369     ($C_{10}H_{16}N_2O_7$; 276 g mol$^{-1}$) were also identified in that study. It is possible that similar products

370     are made following $NO_3$ oxidation of γ-terpinene, and potentially make up the signals detected at

371     *m/z* = 340 and *m/z* = 403, respectively, as shown in Fig. 6. However, the CIMS sensitivity toward

Atmospheric
Chemistry
and Physics
Discussions

372    these products is expected to be relatively small compared to that for the hydroxy nitrates, due to

373    their relatively lower polarity and acidity. Moreover, peroxy nitrates are thermally unstable and

374    their concentrations are likely greatly reduced during transfer through the heated sampling line.

375

376    *3.5.Proposed reaction mechanism*

377    The similarities between the, at first seemingly low, γ-terpinene + $NO_3$-derived $Y_{ONt}$, hydroxy

378    nitrate yield, and $Y_{SOA}$ with those for $NO_3$ + α-pinene are provocative. This suggests the two

379    monoterpenes may undergo very similar degradation pathways following $NO_3$ oxidation, which

380    is not observed with other monoterpenes with a substituted endocyclic double bond [*Fry et al.*,

381    2014]. As such, our mechanistic interpretation, shown in Fig. 8, is analogous to that for the α-

382    pinene + $NO_3$ reaction, as described in the Master Chemical Mechanism (MCM) [*Jenkin et al.*,

383    1997; *Saunders et al.*, 2003]. $NO_3$ will predominately add to the C-3 (unsubstituted) position

384    forming the more stable tertiary alkyl radical. However, to some extent, $NO_3$ may also add to the

385    second carbon forming the less stable secondary alkyl radical, approximately 35% of the time

386    according to the MCM. Oxygen promptly adds to the alkyl radical to form either a tertiary or

387    secondary peroxy radical (ROO·). Excess $NO_2$, due to thermal decomposition of $N_2O_5$, can add

388    to the peroxy radical forming a thermally unstable peroxy nitrate (-$OONO_2$) in equilibrium with

389    the peroxy radical. Subsequent $RO_2$· self- and cross-reactions as well as reaction with $NO_3$ form

390    the alkoxy radical (RO·). The alkoxy radical can subsequently decompose to form a carbonyl

391    nitrate or γ-terpinaldehyde and release $NO_2$. For example, pinonaldehyde is the major $NO_3$

392    oxidation product of α-pinene with reported yields of 62(±4)% [*Wangberg et al.*, 1997] and 71%

393    [*Fry et al.*, 2014]. Given the relatively low yields of SOA, $ON_t$, and hydroxy nitrates observed

394    here for γ-terpinene and the similar double bond character compared to α-pinene, γ-

Atmospheric
Chemistry
and Physics
Discussions

395   terpinaldehyde is likely produced and with similarly high but undetermined yields. Similar

396   results have been reported for the ozonolysis of γ-terpinene, which primarily leads to

397   decomposition and formation of γ-terpinaldehyde with a yield of 58% [*Ng et al.*, 2006].

398   Alternatively, disproportionation, involving a secondary peroxy radical, produces a hydroxy

399   nitrate and a carbonyl compound from the partnering $RO_2$ [*Wangberg et al.*, 1997; *Yeh and*

400   *Ziemann*, 2014; *Ziemann and Atkinson*, 2012]. As we have shown, the experimentally-derived

401   yield for these products is 4%, or roughly 25% of $ON_t$. The remaining organic nitrate species

402   likely contains both carbonyl and hydroperoxy (-OOH) functionalities, and perhaps peroxy

403   nitrates, following $NO_2$ addition to the peroxy radical. A major species detected by our CIMS

404   has an $m/z = 358$, which may represent an $I^-$ adduct with a hydroperoxy nitrate. This product is

405   only produced due to reactions between hydroperoxy radicals ($HO_2\cdot$) and $RO_2\cdot$ [*Ziemann and*

406   *Atkinson*, 2012]. Conceivably, $HO_2\cdot$ is produced in our system from hydrogen abstraction from

407   alkoxy radicals by oxygen [*Wangberg et al.*, 1997].

408        To test the hypothesis that γ-terpinene behaves similarly to α-pinene following reaction

409   with $NO_3$, we ran a simple box model based on the mechanisms for $NO_3$ oxidation of α-pinene as

410   presented in the MCM, and compared the model output with the measured concentrations of γ-

411   terpinene, $NO_2$, and hydroxy nitrates. The model is constrained by the initial and final GC-FID-

412   derived concentrations of γ-terpinene. Since the nitrate radical concentration was not determined

413   experimentally, the concentration of $NO_3$ in the model was determined by adjusting the $N_2O_5$

414   concentration until the fitted concentration change of γ-terpinene matched that which was

415   measured. This approach implicitly assumes γ-terpinene is consumed only from reaction with

416   $NO_3$, which is expected given the orders of magnitude greater reactivity of $NO_3$ compared to the

417   other reactants in our system, which includes $N_2O_5$ and $NO_2$. The results of the model are

Atmospheric
Chemistry
and Physics
Discussions

418    presented in Fig. 9. For comparison, modeled concentrations are plotted along with the measured

419    concentrations of γ-terpinene, $NO_2$, and hydroxy nitrates derived from one of the experiments. At

420    a first approximation, the modeled concentrations appear to be in agreement with those

421    measured, given the semi-quantitative nature of the product, particularly the hydroperoxides.

422    Notably, the good agreement between modeled and measured $NO_2$ concentrations implies large

423    keto–aldehyde yields as $NO_2$ concentrations in the chamber depend on both the initial $N_2O_5$

424    concentration and the decomposition and release of $NO_2$ by the nitrooxy group to form γ-

425    terpinaldehyde. Although not quantified experimentally, qualitative analysis of the CIMS mass

426    spectra indicates the presence of carbonyl and hydroperoxy nitrates, which is consistent with the

427    major ON products expected from the mechanism shown in Fig. 8.

428

429    **4. Atmospheric Implications**

430        The relatively low SOA and ON yields observed here under dry conditions at ambient mass

431    loadings suggests γ-terpinene may not be an important SOA precursor at night, when $NO_3$ can be

432    the dominant oxidant. However, the low saturation vapor pressure of the hydroxy nitrates, which

433    constitute a significant portion of the total ON, and the presence of some highly oxygenated

434    products, further suggests that these molecules are potentially important contributors to SOA

435    mass. At high RH, hydroxy nitrates in the particle phase can enhance SOA formation through

436    acid-catalyzed hydrolysis and oligomerization, and in the presence of sulfates, form organic

437    sulfates [*Liu et al.*, 2012; *Paulot et al.*, 2009; *Rindelaub et al.*, 2016; *Rindelaub et al.*, 2015;

438    *Surratt et al.*, 2008], ultimately affecting the lifetime of $NO_x$ [*Browne and Cohen*, 2012; *F Xiong*

439    *et al.*, 2015]. Furthermore, the transformation of the nitrooxy group to a hydroxyl or sulfate

440  group will alter the hygroscopicity of the particle, making them more effective cloud

441  condensation nuclei [*Suda et al.*, 2014].

442  Although the SOA yields are low, these chamber experiments did not represent all possible

443  reactants that can produce particle phase precursors. Recent work indicates keto–aldehydes are

444  potentially an important source of nitrogen-containing low volatility compounds following their

445  reaction with dimethylamine, serving as precursors to SOA and brown carbon [*Duporté et al.*,

446  2016]. As shown in this study, the keto–aldehyde yield is expected to be large, along with other

447  internal olefinic terpenes. It is also important to note that the keto–aldehyde product, γ-

448  terpinaldehyde, is olefinic. Further homogeneous and multiphase oxidation reactions at the

449  remaining reactive double bond can potentially transform these species into oligomeric lower-

450  volatility oxidation products, adding to the overall SOA burden [*Liggio and Li*, 2008]. In regions

451  such as the northern U.S., where there are greater proportions of polyolefinic monoterpenes

452  [*Geron et al.*, 2000], γ-terpinene may be an important reactive VOC, and thus impact aerosol and

453  local-scale $NO_x$.

454

## 5. Conclusions

456  The total molar ON yield from the $NO_3$ oxidation of γ-terpinene was found to be 14(+3/-2)%.

457  Relatively low particle-phase ON and SOA yields are consistent with previous studies that show

458  SOA yields are generally dependent on the yield of ON. Although γ-terpinene is a diolefin, the

459  ON, hydroxy nitrate, and SOA yields are similar to those for α-pinene oxidation by $NO_3$.

460  Considering the position of the two double bonds, the expected major product is γ-

461  terpinaldehyde, which is considerably more volatile than the ON products. Box model

462  calculations that assume large keto–aldehyde yields are also in agreement with the measured

Atmospheric
Chemistry
and Physics
Discussions
Open Access
EGU

463 concentrations of hydroxy nitrates, suggesting very similar mechanistic behavior to that of α-

464 pinene oxidation. Several gas- and particle-phase ON products have been inferred from mass

465 spectrometry analysis, indicating that $NO_3$ reaction with γ-terpinene may be an important source

466 of ON and dicarbonyl compounds in forest-impacted environments.

467

468 **Author Contributions**

469 J. H. S. and P. B. S. designed the research and wrote the manuscript. J. H. S. performed the yield

470 experiments and analyzed the data. J. H. S. and C. d-P. analyzed the filter samples. L. L. oversaw

471 the analysis of the filter samples. All authors contributed intellectually to the manuscript.

472

473 **Acknowledgements**

Atmospheric
Chemistry
and Physics
Discussions

476 **Tables**

477 Table 1. Initial conditions and yields from individual experiments.

| Date | Seed | $\Delta BVOC$/ ppb | $\Delta ON_g$/ ppb | $\Delta BVOC$/ mol$\times 10^{-5}$ | $\Delta ON_p$/ mol$\times 10^{-6}$ | $Y_{ONg}$ | $Y_{ONp}$ | $\Delta M$/ $\mu g\ m^{-3}$ |
|---|---|---|---|---|---|---|---|---|
| 9/9/15 | None | 229 | 10 | 5.2 | 1.2 | 4% | 2% | 530 |
| 9/17/15 | None | 131 | 16 | 3.0 | 2.5 | 12% | 9% | 272 |
| 9/19/15 | None | 90 | 7 | 2.0 | 1.7 | 7% | 8% | 311 |
| 9/21/15 | None | 214 | 15 | 4.8 | 0.7 | 7% | 2% | 604 |
| 9/23/15 | None | 256 | 21 | 5.8 | 1.7 | 8% | 3% | 534 |
| 9/23/15 | None | 80 | 8 | 1.8 | 0.7 | 10% | 4% | 61 |
| 10/20/15 | $(NH_4)_2SO_4$ | 761 | 90 | 17 | 3.8 | 12% | 2% | 3820 |
| 10/22/15 | $(NH_4)_2SO_4$ | 164 | 31 | 3.7 | 3.5 | 19% | 9% | 578 |
| 10/28/15 | $(NH_4)_2SO_4$ | 47 | 9 | 1.1 | 0.2 | 18% | 2% | 35 |
| 11/09/15 | $(NH_4)_2SO_4$ | 245 | 23 | 5.5 | 0.6 | 10% | 1% | 1157 |
| 11/10/15 | $(NH_4)_2SO_4$ | 66 | 4.5 | 1.5 | 0.6 | 7% | 4% | 162 |
| 11/12/15 | None | 413 | 49 | 9.3 | 2.0 | 12% | 2% | 623 |
| 11/18/15 | None | 408 | 39 | 9.2 | 3.7 | 10% | 4% | 2206 |

478

479 **Figures**
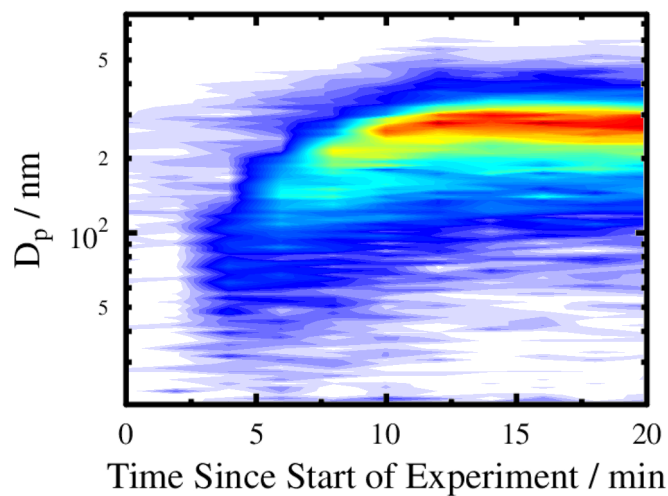


480

481 Figure 1. Example SOA particle diameter ($D_p$) growth curve for γ-terpinene + NO$_3$ in the
482 absence of seed aerosol. The color scale represents aerosol number concentration (cm$^{-3}$).

483
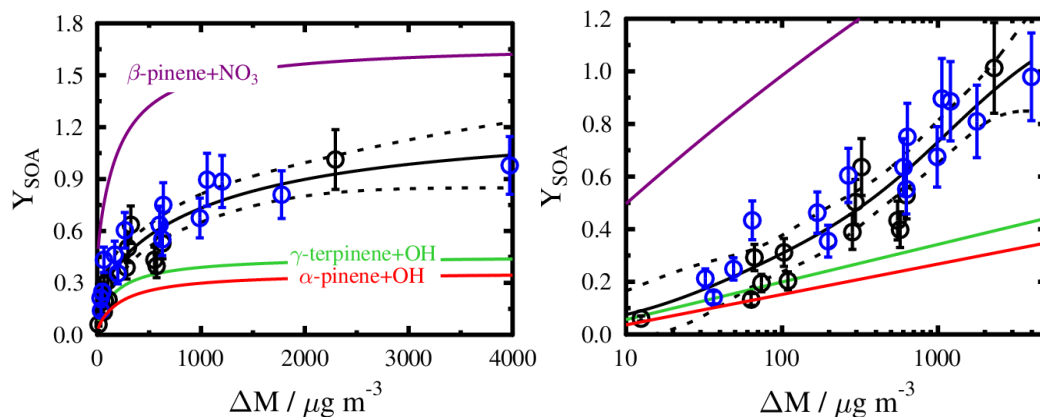
Figure 2. Change in aerosol mass concentration ($\Delta M$) and wall-loss corrected SOA yields ($Y_{SOA}$) from the $NO_3$ oxidation of γ-terpinene in unseeded (black circles) and $(NH_4)_2SO_4$-seeded experiments (blue circles). The data were fitted to a two-product absorptive partitioning model (black curve) and the dashed curves represent the 95% confidence intervals of the fitting function. For comparison, the mass-dependent yield curves of α-pinene and γ-terpinene in the presence of OH are shown in the red and green curves, respectively, and β-pinene + $NO_3$ in purple [*Griffin et al.*, 1999; *A Lee et al.*, 2006]. For clarity, the right panel shows the left panel data on a log scale x axis.

Atmospheric
Chemistry
and Physics
Discussions
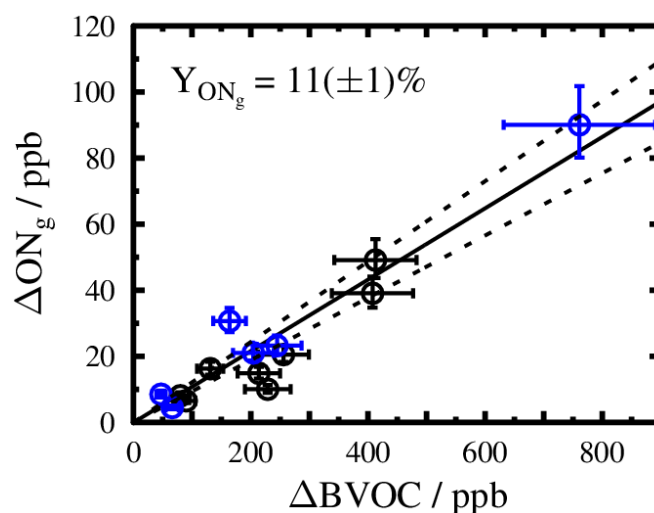
494    Figure 3. Total wall loss- and dilution-corrected gas-phase organic nitrate production ($\Delta ON_g$) as

495    a function of the amount of BVOC consumed ($\Delta BVOC$) for the unseeded (black circles) and

496    ($NH_4)_2SO_4$-seeded experiments (blue circles). Horizontal and vertical error bars represent the

497    uncertainty in the GC-FID and FT-IR calibrations, respectively. The black line shows the linear

498    fit of the data through the origin and the dashed lines indicate the 95% confidence intervals of

499    the fit. The slopes of these lines represent the fractional organic nitrate yield and uncertainty

500    presented in the plot, respectively.
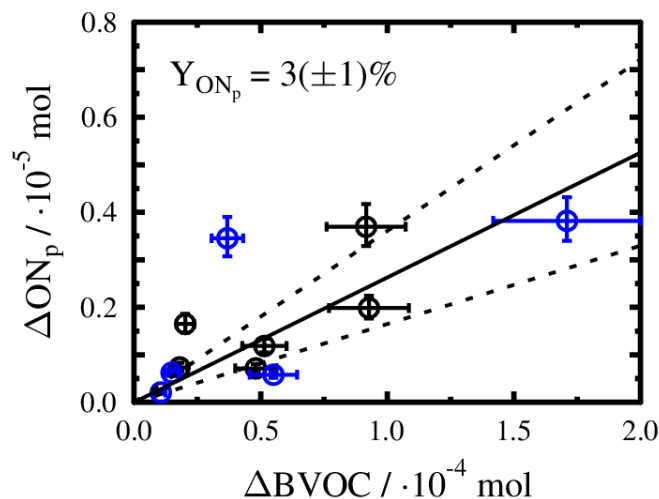


501

502    Figure 4. Total wall loss- and dilution-corrected particle-phase organic nitrate production

503    ($\Delta ON_p$) as a function of the amount of BVOC consumed ($\Delta BVOC$) for the unseeded (black

504    circles) and ($NH_4)_2SO_4$-seeded experiments (blue circles). The presented yield, yield uncertainty,

505    and error bars on the data are derived as in Fig. 3.

25

Atmospheric
Chemistry
and Physics
Discussions

Open Access

EGU
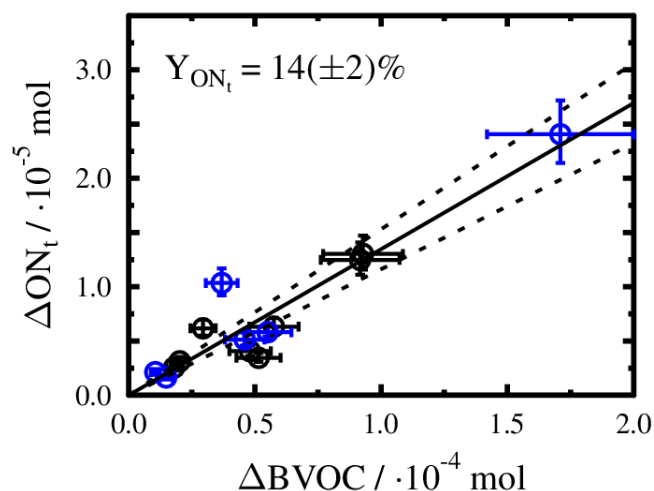


506

507    Figure 5. Total wall loss- and dilution-corrected organic nitrate production ($\Delta ON_t$) as a function

508    of the amount of BVOC consumed ($\Delta BVOC$) for the unseeded (black circles) and $(NH_4)_2SO_4$-

509    seeded experiments (blue circles). The yield, yield uncertainty, and error bars on the data are

510    derived as in Fig. 3.

511
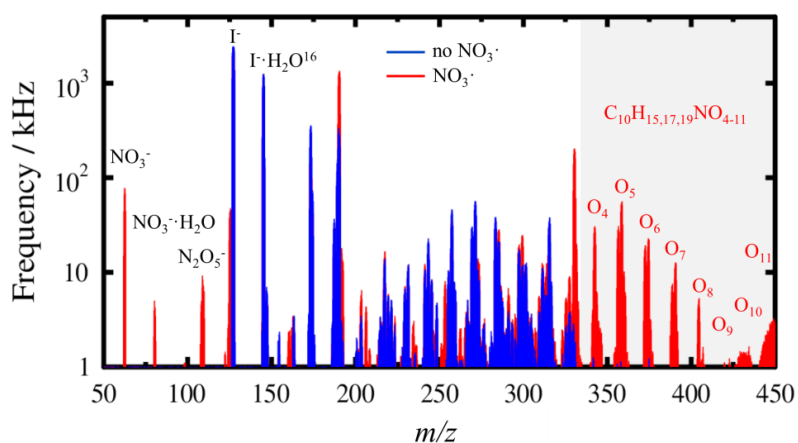


512

513    Figure 6. CIMS mass spectra before (blue) and after $\gamma$-terpinene oxidation by $NO_3$ (red). The

514    shaded region indicates the presence of multifunctional ON compounds with the number of

515    oxygen atoms consistent with the depicted chemical formula.

516
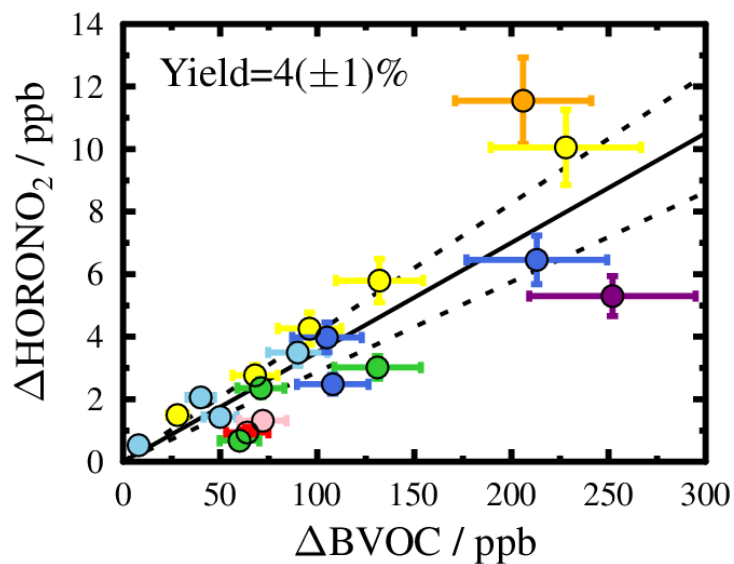
Figure 7. γ-terpinene hydroxy nitrate production ($\Delta HORONO_2$) as a function of the amount of

BVOC consumed ($\Delta BVOC$). Colors represent independent experiments performed on different

days. All of the experiments were conducted in the absence of seed aerosol. The yield, yield

uncertainty, and error bars on the data are derived as in Fig. 3.

Atmospheric
Chemistry
and Physics
Discussions

Open Access

EGU
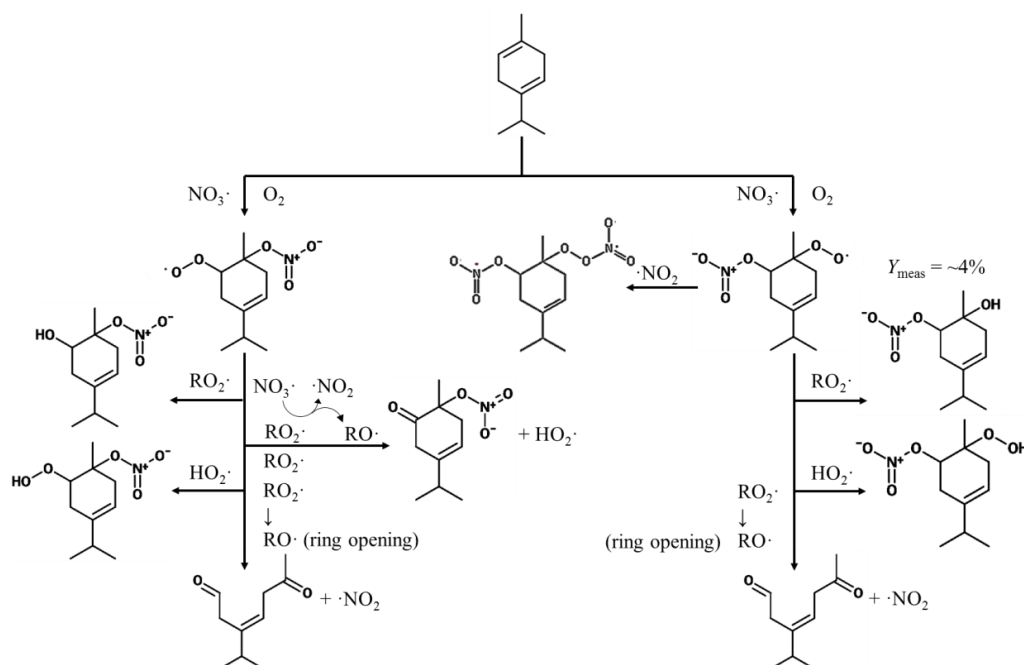


521

522    Figure 8. Proposed initial reaction pathways for the $NO_3$ oxidation of γ-terpinene. For simplicity,

523    only the first-generation oxidation products are shown.
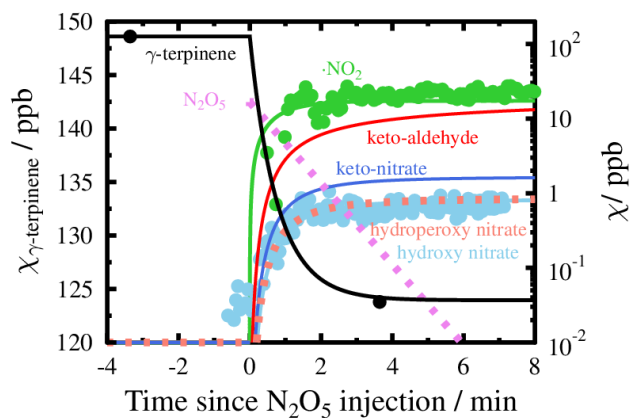


524

525    Figure 9. Time series of experiment indicating measured (circles) and modeled (lines)

526    concentrations of γ-terpinene (black), $N_2O_5$ (dashed violet), $NO_2$ (green), keto-aldehyde (red),

527    keto-nitrate (dark blue), hydroperoxy nitrate (dashed pink), and hydroxy nitrate (light blue). The

528    model is based on the MCM for α-pinene reaction with $NO_3$.

Atmospheric
Chemistry
and Physics
Discussions

# References

Abbatt, J. P. D., A. K. Y. Lee, and J. A. Thornton (2012), Quantifying trace gas uptake to tropospheric aerosol: recent advances and remaining challenges, *Chem. Soc. Rev.*, *41*(19), 6555-6581, doi:10.1039/C2cs35052a.

Ayres, B. R., H. M. Allen, D. C. Draper, S. S. Brown, R. J. Wild, J. L. Jimenez, D. A. Day, P. Campuzano-Jost, W. Hu, J. de Gouw, A. Koss, R. C. Cohen, K. C. Duffey, P. Romer, K. Baumann, E. S. Edgerton, S. Takahama, J. A. Thornton, B. H. Lee, F. Lopez-Hilfiker, C. Mohr, P. O. Wennberg, T. B. Nguyen, A. P. Teng, A. H. Goldstein, K. Olson, and J. L. Fry (2015), Organic nitrate aerosol formation via $NO_3$ + biogenic volatile organic compounds in the southeastern United States, *Atmos. Chem. Phys.*, *15*, 13377-13392, doi:10.5194/acp-15-13377-2015.

Berkemeier, T., M. Ammann, T. F. Mentel, U. Pöschl, and M. Shiraiwa (2016), Organic nitrate contribution to new particle formation and growth in secondary organic aerosols from alpha-pinene ozonolysis, *Environ. Sci. Technol.*, *50*(12), 6334-6342, doi:10.1021/acs.est.6b00961.

Bindu, G., P. R. Nair, S. Aryasree, P. Hegde, and S. Jacob (2016), Pattern of aerosol mass loading and chemical composition over the atmospheric environment of an urban coastal station, *J. Atmos. Sol-Terr. Phy.*, *138-139*, 121-135, doi:10.1016/j.jastp.2016.01.004.

Boyd, C. M., J. Sanchez, L. Xu, A. J. Eugene, T. Nah, W. Y. Tuet, M. I. Guzman, and N. L. Ng (2015), Secondary organic aerosol formation from the beta-pinene + NO3 system: effect of humidity and peroxy radical fate, *Atmos. Chem. Phys.*, *15*, 7497-7522, doi:10.5194/acp-15-7497-2015.

Browne, E. C., and R. C. Cohen (2012), Effects of biogenic nitrate chemistry on the $NO_x$ lifetime in remote continental regions, *Atmos. Chem. Phys.*, *12*, 11917-11932, doi:10.5194/acp-12-11916-2012.

Capouet, M., J.-F. Müller, K. Ceulemans, S. Compernolle, and L. Vereecken (2008), Modeling aerosol formation in alpha-pinene photo-oxidation experiments, *J. Geophys. Res.*, *113*, doi:10.1029/2007JD008995.

Carlton, A. G., and B. J. Turpin (2013), Particle partitioning potential of organic compounds is highest in the Eastern US and driven by anthropogenic water, *Atmos. Chem. Phys.*, *13*(20), 10203-10214, doi:10.5194/acp-13-10203-2013.

Chen, X., D. Hulbert, and P. B. Shepson (1998), Measurement of the organic nitrate yield from OH reaction with isoprene, *J. Geophys. Res.*, *103*(D19), 25563-25568, doi:10.1029/98JD01483.

Compernolle, S., K. Ceulemans, and J.-F. Müller (2011), EVAPORATION: a new vapour pressure estimation method for organic molecules including non-additivity and intramolecular interactions, *Atmos. Chem. Phys.*, *11*, 9431-9450, doi:10.5194/acp-11-9431-2011.

Atmospheric
Chemistry
and Physics
Discussions

Open Access

EGU

604  Darnall, K. R., W. P. L. Carter, A. M. Winer, A. C. Lloyd, and J. N. Pitts (1976), Importance of
605  RO2+NO in alkyl nitrate formation from C4-C6 alkane photooxidations under simulated
606  atmospheric conditions, *J. Phys. Chem.*, *80*(17), 1948-1950, doi:10.1021/j100558a029.

607  Donahue, N. M., S. A. Epstein, S. N. Pandis, and A. L. Robinson (2011), A two-dimensional
608  volatility basis set: 1. organic-aerosol mixing thermodynamics, *Atmos. Chem. Phys.*, *11*, 3308-
609  3318, doi:10.5194/acp-11-3303-2011.

610  Duporté, G., J. Parshintsev, L. M. F. Barreira, K. Hartonen, M. Kulmala, and M. L. Riekkola
611  (2016), Nitrogen-containing low volatile compounds from pinonaldehyde-dimethylamine
612  reaction in the atmosphere: a laboratory and field study, *Environ. Sci. Technol.*, *50*(9), 4693-
613  4700, doi:10.1021/acs.est.6b00270.

614  Fry, J. L., D. C. Draper, K. C. Barsanti, J. N. Smith, J. Ortega, P. M. Winkler, M. J. Lawler, S. S.
615  Brown, P. M. Edwards, R. C. Cohen, and L. Lee (2014), Secondary organic aerosol formation
616  and organic nitrate yield from $NO_3$ oxidation of biogenic hydrocarbons, *Environ. Sci. Technol.*,
617  *48*, 11944-11953, doi:10.1021/es502204x.

618  Fry, J. L., A. Kiendler-Scharr, A. W. Rollins, P. J. Wooldridge, S. S. Brown, H. Fuchs, W. Dube,
619  A. Mensah, M. dal Maso, R. Tillmann, H. P. Dorn, T. Brauers, and R. C. Cohen (2009), Organic
620  nitrate and secondary organic aerosol yield from $NO_3$ oxidation of beta-pinene evaluated using a
621  gas-phase kinetics/aerosol partitioning model, *Atmos. Chem. Phys.*, *9*, 1431-1449,
622  doi:10.5194/acp-9-2009-1431-1449.

623  Geron, C., R. Rasmussen, R. Arnts, and A. B. Guenther (2000), A review and synthesis of
624  monoterpene speciation from forests in the United States, *Atmos. Environ.*, *34*(11), 1761-1781,
625  doi:10.1016/S1352-2310(99)00364-7.

626  Glasius, M., and A. H. Goldstein (2016), Recent discoveries and future challenges in
627  atmospheric  organic  chemistry,  *Environ.  Sci.  Technol.*,  *50*(6),  2754-2764,
628  doi:10.1021/acs.est.5b05105.

629  Goldstein, A. H., and I. E. Galbally (2007), Known and unexplored organic constituents in the
630  Earth's atmosphere, *Environ. Sci. Technol.*, *41*(5), 1514-1521, doi:10.1021/es072476p.

631  Griffin, R. J., D. R. Cocker III, R. C. Flagan, and J. H. Seinfeld (1999), Organic aerosol
632  formation from the oxidation of biogenic hydrocarbons, *J. Geophys. Res.*, *104*(D3), 3555-3567,
633  doi:10.1029/1998JD100049.

634  Grossenbacher, J. W., D. J. Barket, P. B. Shepson, M. A. Carroll, K. Olszyna, and E. Apel
635  (2004), A comparison of isoprene nitrate concentrations at two forest-impacted sites, *J Geophys
636  Res-Atmos*, *109*(D11), doi:10.1029/2003jd003966.

637  Guenther, A. (2002), The contribution of reactive carbon emissions from vegetation to the
638  carbon balance of terrestrial ecosystems, *Chemosphere*, *49*(8), 837-844, doi:10.1016/S0045-
639  6535(02)00384-3.

Atmospheric
Chemistry
and Physics
Discussions

640 Guenther, A., C. N. Hewitt, D. Erickson, R. Fall, C. Geron, T. Graedel, P. Harley, L. Klinger, M.
641 Lerdau, W. A. Mckay, T. Pierce, B. Scholes, R. Steinbrecher, R. Tallamraju, J. Taylor, and P.
642 Zimmerman (1995), A global model of natural volatile organic compound emissions, *J.
643 Geophys. Res.*, *100*(D5), 8873-8892, doi:10.1029/94JD02950.

644 Hallquist, M., J. C. Wenger, U. Baltensperger, Y. Rudich, D. Simpson, M. Claeys, J. Dommen,
645 N. M. Donahue, C. George, A. H. Goldstein, and J. F. Hamilton (2009), The formation,
646 properties and impact of secondary organic aerosol: current and emerging issues, *Atmos. Chem.
647 Phys.*, *9*, 5155-5236, doi:10.5194/acp-9-5155-2009.

648 Hao, L. Q., S. Romakkaniemi, P. Yli-Pirila, J. Joutsensaari, A. Kortelainen, J. H. Kroll, P.
649 Miettinen, P. Vaattovaara, P. Tiitta, A. Jaatinen, M. K. Kajos, J. K. Holopainen, J. Heijari, J.
650 Rinne, M. Kulmala, D. R. Worsnop, J. N. Smith, and A. Laaksonen (2011), Mass yields of
651 secondary organic aerosols from the oxidation of alpha-pinene and real plant emissions, *Atmos.
652 Chem. Phys.*, *11*, 1367-1378, doi:10.5194/acp-11-1367-2011.

653 Hoyle, C. R., M. Boy, N. M. Donahue, J. L. Fry, M. Glasium, A. Guenther, A. G. Hallar, K. Huff
654 Hartz, M. D. Petters, T. Petaja, T. Rosenoern, and A. P. Sullivan (2011), A review of the
655 anthropogenic influence on biogenic secondary organic aerosol, *Atmos. Chem. Phys.*, *11*, 321-
656 343, doi:10.5194/acp-11-321-2011.

657 Jacobs, M. I., W. J. Burke, and M. J. Elrod (2014), Kinetics of the reactions of isoprene-derived
658 hydroxynitrates: gas phase epoxide formation and solution phase hydrolysis, *Atmos. Chem.
659 Phys.*, *14*, 8933-8946, doi:10.5194/acp-14-8933-2014.

660 Jenkin, M. E., S. M. Saunders, and M. J. Pilling (1997), The tropospheric degradation of volatile
661 organic compounds: A protocol for mechanism development, *Atmos Environ*, *31*(1), 81-104,
662 doi:10.1016/S1352-2310(96)00105-7.

663 Kokkola, H., P. Yli-Pirila, M. Vesterinen, H. Korhonen, H. Keskinen, S. Romakkaniemi, L. Hao,
664 A. Kortelainen, J. Joutsensaari, D. R. Worsnop, A. Virtanen, and K. E. J. Lehtinen (2014), The
665 role o flow volatile organics on secondary organic aerosol formation, *Atmos. Chem. Phys.*, *14*,
666 1689-1700, doi:10.5194/acp-14-1689-2014.

667 Kroll, J. H., and J. H. Seinfeld (2008), Chemistry of secondary organic aerosol: formation and
668 evolution of low-volatility organics in the atmosphere, *Atmos. Environ.*, *42*(16), 3593-3624,
669 doi:10.1016/j.atmosenv.2008.01.003.

670 Lee, A., A. H. Goldstein, J. H. Kroll, N. L. Ng, V. Varutbangkul, R. C. Flagan, and J. H. Seinfeld
671 (2006), Gas-phase products and secondary aerosol yields from the photooxidation of 16 different
672 terpenes, *J. Geophys. Res.*, *111*, D17305, doi:10.1029/2006JD007050.

673 Lee, B. H., C. Mohr, F. D. Lopez-Hilfiker, A. Lutz, M. Hallquist, L. Lee, P. Romer, R. C. Cohen,
674 S. Lyer, T. Kurten, W. Hu, D. A. Day, P. Campuzano-Jost, J. L. Jimenez, L. Xu, N. L. Ng, H.
675 Guo, R. J. Weber, R. J. Wilde, S. S. Brown, A. Koss, J. de Gouw, K. Olson, A. H. Goldstein, R.
676 Seco, S. Kim, K. M. McAvey, P. B. Shepson, T. K. Starn, K. Baumann, E. S. Edgerton, J. Liu, J.
677 E. Shilling, D. O. Miller, W. Brune, S. Schobesberger, E. L. D'Ambro, and J. A. Thornton
678 (2016), Highly functionalized organic nitrates in the southeast United States: contribution to

Atmospheric
Chemistry
and Physics
Discussions

679   secondary organic aerosol and reactive nitrogen budgets, *Proc. Nat. Acad. Sci.*, *113*(6), 1516-
680   1521, doi:10.1073/pnas.1508108113.

681   Liggio, J., and S.-M. Li (2008), Reversible and irreversible processing of biogenic olefins on
682   acidic aerosols, *Atmos. Chem. Phys.*, *8*, 2039-2055, doi:10.5194/acp-8-2039-2008.

683   Liu, S., J. E. Shilling, C. Song, N. Hiranuma, R. A. Zaveri, and L. M. Russell (2012), Hydrolysis
684   of organonitrate functional groups in aerosol particles, *Aerosol Sci Tech*, *46*, 1359-1369,
685   doi:10.1080/02786826.2012.716175.

686   Lockwood, A. L., P. B. Shepson, M. N. Fiddler, and M. Alaghmand (2010), Isoprene nitrates:
687   preparation, separation, identification, yields, and atmospheric chemistry, *Atmos. Chem. Phys.*,
688   *10*, 6169-6178, doi:10.5194/acp-10-6169-2010.

689   Martinez, E., B. Cabañas, A. Aranda, P. Martin, and S. Salgado (1999), Absolute rate
690   coefficients for the gas-phase reactions of $NO_3$ radical with a series of monoterpenes at T=298 to
691   433 K, *J. Atmos. Chem.*, *33*(3), 265-282, doi:10.1023/A:1006178530211.

692   Ng, N. L., J. H. Kroll, M. D. Keywood, R. Bahreini, V. Varutbangkul, R. C. Flagan, J. H.
693   Seinfeld, A. Lee, and A. H. Goldstein (2006), Contribution of first- versus second-generation
694   products to secondary organic aerosols formed in the oxidation of biogenic hydrocarbons,
695   *Environ Sci Technol*, *40*(7), 2283-2297, doi:10.1021/es052269u.

696   Odum, J. R., T. Hoffmann, F. Bowman, D. Collins, R. C. Flagan, and J. H. Seinfeld (1996),
697   Gas/particle partitioning and secondary organic aerosol yields, *Environ. Sci. Technol.*, *30*.

698   Pankow, J. F., and W. E. Asher (2008), SIMPOL.1: A simple group contribution method for
699   predicting vapor pressures and enthalpies of vaporization of multifunctional organic compounds,
700   *Atmos. Chem. Phys.*, *8*(10), 2773-2796, doi:10.5194/acp-8-2773-2008.

701   Paulot, F., J. D. Crounse, H. G. Kjaergaard, J. H. Kroll, J. H. Seinfeld, and P. O. Wennberg
702   (2009), Isoprene photooxidation: new insights into the production of acids and organic nitrates,
703   *Atmos. Chem. Phys.*, *9*, 1479-1501, doi:10.5194/acp-9-1479-2009.

704   Perring, A. E., A. Wisthaler, M. Graus, P. J. Wooldridge, A. L. Lockwood, L. H. Mielke, P. B.
705   Shepson, A. Hansel, and R. C. Cohen (2009), A product study of the isoprene+$NO_3$ reaction,
706   *Atmos. Chem. Phys.*, *9*, 4945-4956, doi:10.5194/acp-9-4945-2009.

707   Pratt, K. A., L. H. Mielke, P. B. Shepson, A. M. Bryan, A. L. Steiner, J. Ortega, R. Daly, D.
708   Helmig, C. S. Vogel, S. Griffith, S. Dusanter, P. S. Stevens, and M. Alaghmand (2012),
709   Contributions of individual reactive biogenic volatile organic compounds to organic nitrates
710   above a mixed forest, *Atmos. Chem. Phys.*, *12*, 10125-10143, doi:10.5194/acp-12-10125-2012.

711   Pye, H. O. T., D. J. Luecken, L. Xu, C. M. Boyd, N. L. Ng, K. R. Baker, B. R. Ayres, J. O. Bash,
712   K. Baumann, W. P. L. Carter, E. S. Edgerton, J. L. Fry, W. T. Hutzell, D. B. Schwede, and P. B.
713   Shepson (2015), Modeling the current and future roles of particulate organic nitrates in the
714   Southeastern United States, *Environ. Sci. Technol.*, *49*(24), 14195-14203,
715   doi:10.1021/acs.est.5b03738.

Atmospheric
Chemistry
and Physics
Discussions

716   Riipinen, I., T. Yli-Juuti, J. R. Pierce, T. Petaja, D. R. Worsnop, M. Kulmala, and N. M.
717   Donahue (2012), The contribution of organics to atmospheric nanoparticle growth, *Nature
718   Geoscience*, *5*, 453-458, doi:10.1038/ngeo1499.

719   Rindelaub, J. D., C. H. Borca, M. A. Hostetler, J. H. Slade, M. A. Lipton, L. V. Slipchenko, and
720   P. B. Shepson (2016), The acid-catalyzed hydrolysis of an α-pinene-derived organic nitrate:
721   kinetics, products, reaction mechanisms, and atmospheric impact, *Atmos. Chem. Phys.*, *16*,
722   15425-15432, doi:10.5194/acp-16-15425-2016.

723   Rindelaub, J. D., K. M. McAvey, and P. B. Shepson (2015), The photochemical production of
724   organic nitrates from alpha-pinene and loss via acid-dependent particle phase hydrolysis, *Atmos.
725   Environ.*, *100*, 193-201, doi:10.1016/j.atmosenv.2014.10.010.

726   Rollins, A. W., E. C. Browne, K. E. Min, S. E. Pusede, P. J. Wooldridge, D. R. Gentner, A. H.
727   Goldstein, S. Liu, D. A. Day, L. M. Russell, and R. C. Cohen (2012), Evidence for $NO_x$ control
728   over nighttime SOA formation, *Science*, *337*, doi:10.1126/science.1221520.

729   Rollins, A. W., J. L. Fry, J. F. Hunter, J. H. Kroll, D. R. Worsnop, S. W. Singaram, and R. C.
730   Cohen (2010a), Elemental analysis of aerosol organic nitrates with electron ionization high-
731   resolution mass spectrometry, *Atmos. Meas. Tech.*, *3*(1), 301-310, doi:10.5194/amt-3-301-2010.

732   Rollins, A. W., J. D. Smith, K. R. Wilson, and R. C. Cohen (2010b), Real time in situ detection
733   of organic nitrates in atmospheric aerosols, *Environ. Sci. Technol.*, *44*, 5540-5545,
734   doi:10.1021/es100926x.

735   Saunders, S. M., M. E. Jenkin, R. G. Derwent, and M. J. Pilling (2003), Protocol for the
736   development of the Master Chemical Mechanism, MCM v3 (Part A): tropospheric degradation
737   of non-aromatic volatile organic compounds, *Atmos Chem Phys*, *3*, 161-180, doi:10.5194/acp-3-
738   161-2003.

739   Shepson, P. B., E. Mackay, and K. Muthuramu (1996), Henry's law constants and removal
740   processes for several atmospheric beta-hydroxy alkyl nitrates, *Environ Sci Technol*, *30*(12),
741   3618-3623, doi:10.1021/Es960538y.

742   Shiraiwa, M., and J. H. Seinfeld (2012), Equilibration timescale of atmospheric secondary
743   organic aerosol partitioning, *Geophys Res Lett*, *39*, doi:10.1029/2012gl054008.

744   Spittler, M., I. Barnes, I. Bejan, K. J. Brockmann, T. Benter, and K. Wirtz (2006), Reactions of
745   NO3 radicals with limonene and alpha-pinene: Product and SOA formation, *Atmos Environ*, *40*,
746   S116-S127, doi:10.1016/j.atmosenv.2005.09.093.

747   Spracklen, D. V., K. S. Carslaw, U. Pöschl, A. Rap, and P. M. Forster (2011), Global cloud
748   condensation nuclei influenced by carbonaceous combustion aerosol, *Atmos. Chem. Phys.*, *11*,
749   9067-9087, doi:10.5194/acp-11-9067-2011.

750   Squire, O. J., A. T. Archibald, P. T. Griffiths, M. E. Jenkin, D. Smith, and J. A. Pyle (2015),
751   Influence of isoprene chemical mechanisms on modelled changes in tropospheric ozone due to

Atmospheric
Chemistry
and Physics
Discussions

752   climate and land use over the 21st century, *Atmos. Chem. Phys.*, *15*, 5123-5143,
753   doi:10.5194/acp-15-5123-2015.

754   Stocker, T. F., D. Qin, G. K. Plattner, M. Tignor, S. K. Allen, J. Boschung, A. Nauels, Y. Xia, V.
755   Bex, and P. M. Midgley (2013), *Climate Change 2013: the Physical Science Basis, contribution*
756   *of Working Group 1 to the Fifth  Assessment Report of the Intergovernmental Panel on Climate*
757   *Change*, Cambridge University Press, Cambridge, UK and New York, NY, USA.

758   Suda, S. R., M. D. Petters, G. K. Yeh, C. Strollo, A. Matsunaga, A. Faulhaber, P. J. Ziemann, A.
759   J. Prenni, C. M. Carrico, R. C. Sullivan, and S. M. Kreidenweis (2014), Influence of functional
760   groups on organic aerosol cloud condensation nucleus activity, *Environ. Sci. Technol.*, *48*(17),
761   10182-10190, doi:10.1021/es502147y.

762   Surratt, J. D., Y. Gomez-Gonzalez, A. W. H. Chan, R. Vermeylen, M. Shahgholi, and T. E.
763   Kleindienst (2008), Organosulfate formation in biogenic secondary organic aerosol, *J. Phys.*
764   *Chem. A*, *112*, 8345-8378, doi:10.1021/jp802310p.

765   Tsigaridis, K., and M. Kanakidou (2007), Secondary organic aerosol importance in the future
766   atmosphere, *Atmos. Environ.*, *41*, 4682-4692, doi:10.1016/j.atmosenv.2007.03.045.

767   Valorso, R., B. Aumont, M. Camredon, T. Raventos-Duran, C. Mouchel-Vallon, N. L. Ng, J. H.
768   Seinfeld, J. Lee-Taylor, and S. Madronich (2011), Explicit modelling of SOA formation from α-
769   pinene photooxidation: sensitivity to vapour pressure estimation, *Atmos. Chem. Phys.*, *11*, 6895-
770   6910, doi:10.5194/acp-11-6895-2011.

771   von Schneidemesser, E., P. S. Monks, J. D. Allan, L. Bruhwiler, P. Forster, D. Fowler, A. Lauer,
772   W. T. Morgan, P. Paasonen, M. Righi, K. Sindelarova, and M. A. Sutton (2015), Chemistry and
773   the linkages between air quality and climate change, *Chem. Rev.*, *115*(10), 3856-3897,
774   doi:10.1021/acs.chemrev.5b00089.

775   Wangberg, I., I. Barnes, and K.-H. Becker (1997), Product and mechanistic study of the reaction
776   of NO3 radicals with alpha-pinene, *Environ. Sci. Technol.*, *31*, 2130-2135,
777   doi:10.1021/es960958n.

778   Xiong, F., K. M. McAvey, K. A. Pratt, C. J. Groff, M. A. Hostetler, M. A. Lipton, T. K. Starn, J.
779   V. Seeley, S. B. Bertman, A. P. Teng, J. D. Crounse, T. B. Nguyen, P. O. Wennberg, P. K.
780   Misztal, A. H. Goldstein, A. B. Guenther, A. R. Koss, K. F. Olson, J. A. de Gouw, K. Baumann,
781   E. S. Edgerton, P. A. Feiner, L. Zhang, D. O. Miller, W. H. Brune, and P. B. Shepson (2015),
782   Observations of isoprene hydroxynitrates in the southeastern United States and implications for
783   the fate of NO$_x$, *Atmos. Chem. Phys.*, *15*, 11257-11272, doi:10.5194/acp-15-11257-2015.

784   Xiong, F. L. Z., C. H. Borca, L. V. Slipchenko, and P. B. Shepson (2016), Photochemical
785   degradation of isoprene-derived 4,1-nitrooxy enal, *Atmos Chem Phys*, *16*(9), 5595-5610,
786   doi:10.5194/acp-16-5595-2016.

787   Xu, L., S. Suresh, H. Guo, R. J. Weber, and N. L. Ng (2015), Aerosol characterization over the
788   southeastern United States using high-resolution aerosol mass spectrometry: spatial and seasonal

789    variation of aerosol composition and sources with a focus on organic nitrates, *Atmos Chem Phys*,
790    *15*(13), 7307-7336, doi:10.5194/acp-15-7307-2015.

791    Yeh, G. K., and P. J. Ziemann (2014), Alkyl nitrate formation from the reactions of $C_8$-$C_{14}$ *n*-
792    alkanes with OH radicals in the presence of $NO_x$: measured yields with essential corrections for
793    gas-wall partitioning, *J. Phys. Chem. A*, *118*, 8147-8157, doi:10.1021/jp500631v.

794    Ziemann, P. J., and R. Atkinson (2012), Kinetics, products, and mechanisms of secondary
795    organic aerosol formation, *Chem. Soc. Rev.*, *41*, 6582-6605, doi:10.1039/C2CS35122F.

796